Light scattering by a periodically time-modulated object of arbitrary shape: the extended boundary condition method

Nikolaos Stefanou,[1] Ioannis Stefanou,[1] Evangelos Almpanis,[1,2,*] Nikolaos Papanikolaou,[2] Puneet Garg,[3] and Carsten Rockstuhl[3,4]

[1]*Section of Condensed Matter Physics, National and Kapodistrian University of Athens, Panepistimioupolis, GR-157 84 Athens, Greece*
[2]*Institute of Nanoscience and Nanotechnology, NCSR "Demokritos," Patriarchou Gregoriou and Neapoleos Str., Ag. Paraskevi, GR-153 10 Athens, Greece*
[3]*Institute of Theoretical Solid State Physics, Karlsruhe Institute of Technology, Wolfgang-Gaede-Str. 1, D-76131 Karlsruhe, Germany*
[4]*Institute of Nanotechnology, Karlsruhe Institute of Technology, P.O. Box 3640, D-76021 Karlsruhe, Germany*
**ealmpanis@gmail.com*

A proper generalization of the extended boundary condition method to calculate the transition matrix, T, for electromagnetic scattering from a homogeneous and isotropic body of arbitrary shape, characterized by a periodically time-varying electric permittivity, is presented. The application of the method on a specific example of a spheroidal dielectric particle confirms that time modulation induces strong inelastic scattering, accompanied by energy transfer between the scatterer and the light field, when the difference of the incident wave frequency to a particle optical resonance matches an integer multiple of the modulation frequency. Moreover, it is shown that, for nonspherical scatterers, these effects can be selectively tuned by external means such as the polarization and the propagation direction of the incident light beam. The method is readily implementable in available dynamic multiple-scattering computer codes, and, because of its versatility and computational efficiency, it can offer new opportunities for studying more complex time-varying photonic structures.

1. INTRODUCTION

The extended boundary condition method (EBCM), formulated originally by Waterman [1,2] and later by Barber and Yeh [3], has gained considerable popularity as a versatile tool to calculate the on-shell transition matrix, T, in various applications involving electromagnetic (EM) scattering by nonspherical objects [4–9]. The approach proves efficient, particularly when dealing with size parameters and deviations from spherical shape that are not excessively large [10,11]. In particular, the EBCM algorithm was successfully implemented into the layer multiple scattering (LMS) method [12] and subsequently applied in the study and analysis of various photonic structures [13–19].

The EBCM assumes monochromatic waves of angular frequency ω and employs an expansion of the scattered and the incident fields into transverse vector spherical partial waves [20]—outgoing: $\mathbf{H}_{Hlm}(q_\mathrm{h},\mathbf{r})=h_l^+(q_\mathrm{h}r)\mathbf{X}_{lm}(\mathbf{r})$, $\mathbf{H}_{Elm}(q_\mathrm{h},\mathbf{r})=\frac{i}{q_\mathrm{h}}\nabla\times\mathbf{H}_{Hlm}(q_\mathrm{h},\mathbf{r})$ and regular ones: $\mathbf{J}_{Hlm}(q_\mathrm{h},\mathbf{r})=j_l(q_\mathrm{h}r)\mathbf{X}_{lm}(\mathbf{r})$, $\mathbf{J}_{Elm}(q_\mathrm{h},\mathbf{r})=\frac{i}{q_\mathrm{h}}\nabla\times\mathbf{J}_{Hlm}(q_\mathrm{h},\mathbf{r})$, respectively, where h_l^+ (j_l) are the spherical Hankel (Bessel) functions; $q_\mathrm{h}=\omega\sqrt{\epsilon_\mathrm{h}\mu_\mathrm{h}}/c$, with c being the velocity of light in vacuum, is the wavenumber in the host region (outside the object), which is characterized by a relative electric permittivity ϵ_h and magnetic permeability μ_h; and $\mathbf{X}_{lm}(\mathbf{r})$ are the vector spherical harmonics, with $l=1,2,\ldots$ and $m=-l,-l+1,\ldots,l$. Similar expansions into regular vector spherical partial waves are also employed for the field inside the object at the given frequency. The polarization mode, $P=H,E$, characterizes multipoles of magnetic and electric type, which are also termed transverse electric (TE) and transverse magnetic (TM), respectively [20].

In recent years, EM propagation and scattering in time-varying media [21] and, in particular, in media subject to a periodic time modulation have been receiving increasing attention in the general context of periodically driven Floquet time crystals [22–26] and attract considerable interest for novel applications in nonreciprocal photonic devices (see, e.g., [27] and references therein), as well as in the design of active optical metamaterials [28–30], dynamically controlled metasurfaces [31–35], and spatiotemporal diffraction gratings [36]. The intense research activity in this field motivated, also, theoretical work on EM scattering by time-modulated isolated objects,

revealing intriguing phenomena such as strong inelastic scattering, energy transfer, parametric Mie resonances, and directional amplification [37–42]. What is more, the single-particle T matrix, evaluated in these studies, can be easily implemented in available multiple-scattering methods, opening up new opportunities for studying more complex dynamic photonic configurations with temporally modulated building units [43,44]. However, T matrix codes have been developed so far only for spherical time-modulated bodies, which, in some sense, limits the possibilities of exploring wider classes of dynamic photonic structures, with more degrees of freedom to manipulate EM waves. The purpose of the present paper is, following a rigorous full electrodynamic Floquet approach, to present an extention of the EBCM to homogeneous and isotropic scatterers of arbitrary shape, characterized by an electric permittivity that varies periodically in time. The associated T matrix is similar to, but of greater dimension than, that in the static case and can be readily implemented into the recently developed dynamic versions of the LMS computational methodology [43,44].

The remainder of the paper is organized as follows. Section 2 is devoted to the development of our theoretical method. We derive a system of linear algebraic equations, which yields the T matrix of a nonspherical scatterer subject to a periodic time modulation. Our formulation reduces to the well-known results for the unmodulated nonspherical scatterer [12] and the modulated sphere [37] in the appropriate limits. Moreover, we discuss certain aspects related to the numerical implementation and the convergence of the method. In Section 3, we demonstrate the applicability of our dynamic EBCM to the particular case of a periodically driven spheroidal germanium particle and analyze some remarkable effects, in particular strong, resonant inelastic light scattering and energy transfer from (to) the modulated particle to (from) the EM field. It is worth noting that these effects can be selectively tuned by external means, such as the polarization and the propagation direction of the incident light beam, which is not the case for spherical scatterers. We provide a consistent interpretation of the underlying physics and highlight the role of symmetry invoking group theory. Our main findings are summarized in Section 4.

2. FORMULATION AND METHOD

We assume a single homogeneous body, occupying a region $V_{\rm in}$ bounded by a closed surface S and embedded in an otherwise homogeneous, isotropic, and nonabsorbing medium, characterized by a relative electric permittivity $\epsilon_{\rm h}$ and magnetic permeability $\mu_{\rm h}$. The body is centered at the origin of coordinates and has a nondispersive permeability μ and a permittivity that varies periodically in time, $\epsilon(t)=\epsilon(t+T)$.

The electric component of the EM field inside the body ($\mathbf{r}\in V_{\rm in}$) has the general form of

$$\mathbf{E}_{\rm in}(\mathbf{r},t)=\mathrm{Re}\left[\sum_{n=-N}^{N}\mathbf{E}_{\rm in}^{(n)}(\mathbf{r})\exp(-i\omega_n t)\right], \tag{1}$$

with $\omega_n=\omega-n\Omega$ ($\Omega\equiv 2\pi/T$) and

$$\mathbf{E}_{\rm in}^{(n)}(\mathbf{r})=\sum_{\nu=-N}^{N}\sum_{L}a_{L\nu}v_{n;\nu}\mathbf{J}_L(q_\nu,\mathbf{r}), \tag{2}$$

where $v_{n;\nu}$ and q_ν are the components of the νth eigenvector and the eigenvalue, respectively, of the product matrix $\mathbf{DE}$, with $\mathbf{D}=\mathrm{diag}(\mu\omega_{-N}^2/c^2,\mu\omega_{-N+1}^2/c^2,\ldots,\mu\omega_N^2/c^2)$ and $\mathbf{E}$ being the Toeplitz matrix of the Fourier coefficients of $\epsilon(t)$, with elements $E_{nn'}=1/T\int_0^T \mathrm{d}t\epsilon(t)\exp[-i(n-n')\Omega t]$ [37], which determine the νth polychromatic eigenmode of the EM field in the (infinite) time-modulated medium. $a_{L\nu}$ are amplitudes of the corresponding spherical wave components to be determined from imposing interface conditions. The latter are characterized by a collective index $L\equiv Plm$, with $P=H,E$ denoting the polarization.

We consider an incident field consisting of a sum of monochromatic waves of angular frequencies ω_n and corresponding partial spherical wave amplitudes $a_L^{0(n)}$,

$$\mathbf{E}_{\rm inc}(\mathbf{r},t)=\mathrm{Re}\left[\sum_{n=-N}^{N}\mathbf{E}_{\rm inc}^{(n)}(\mathbf{r})\exp(-i\omega_n t)\right], \tag{3}$$

with

$$\mathbf{E}_{\rm inc}^{(n)}(\mathbf{r})=\sum_{L}a_L^{0(n)}\mathbf{J}_L(q_{{\rm h}n},\mathbf{r}), \tag{4}$$

where $q_{{\rm h}n}=\omega_n\sqrt{\epsilon_{\rm h}\mu_{\rm h}}/c$, which, scattered by the object, generates a series of monochromatic outgoing waves so that the scattered field has the following form:

$$\mathbf{E}_{\rm sc}(\mathbf{r},t)=\mathrm{Re}\left[\sum_{n=-N}^{N}\mathbf{E}_{\rm sc}^{(n)}(\mathbf{r})\exp(-i\omega_n t)\right], \tag{5}$$

with

$$\mathbf{E}_{\rm sc}^{(n)}(\mathbf{r})=\sum_{L}a_L^{+(n)}\mathbf{H}_L(q_{{\rm h}n},\mathbf{r}), \tag{6}$$

where $a_L^{+(n)}$ represents the corresponding partial spherical wave amplitudes. Therefore, in the infinite region exterior to the object ($\mathbf{r}\in V_{\rm out}$), the total field is the sum of the incident plus the scattered fields, i.e.,

$$\mathbf{E}_{\rm out}(\mathbf{r},t)=\mathrm{Re}\left[\sum_{n=-N}^{N}\mathbf{E}_{\rm out}^{(n)}(\mathbf{r})\exp(-i\omega_n t)\right], \tag{7}$$

with

$$\mathbf{E}_{\rm out}^{(n)}(\mathbf{r})=\mathbf{E}_{\rm inc}^{(n)}(\mathbf{r})+\mathbf{E}_{\rm sc}^{(n)}(\mathbf{r}). \tag{8}$$

It follows from Maxwell's equations that, for $\mathbf{r}\in V_{\rm out}$,

$$\nabla\times\nabla\times\mathbf{E}_{\rm out}^{(n)}(\mathbf{r})=q_{{\rm h}n}^2\mathbf{E}_{\rm out}^{(n)}(\mathbf{r}). \tag{9}$$

The associated Green's dyadic, which satisfies the equation

$$\left[\nabla\times\nabla\times-q_{{\rm h}n}^2\right]\overleftrightarrow{G}(\mathbf{r},\mathbf{r}';\omega_n)=\overleftrightarrow{I}\delta(\mathbf{r}-\mathbf{r}'), \tag{10}$$

can be expanded into vector spherical waves as follows:

$$\overleftrightarrow{G}(\mathbf{r},\mathbf{r}';\omega_n)=iq_{{\rm h}n}\sum_{L}\left[\bar{\mathbf{H}}_L(q_{{\rm h}n},\mathbf{r})\mathbf{J}_L(q_{{\rm h}n},\mathbf{r}')\Theta(r-r')\right.$$
$$\left.+\bar{\mathbf{J}}_L(q_{{\rm h}n},\mathbf{r})\mathbf{H}_L(q_{{\rm h}n},\mathbf{r}')\Theta(r'-r)\right],\quad \text{for } \mathbf{r}\neq\mathbf{r}', \tag{11}$$

where Θ is the unit step function and the overbar denotes complex conjugation of the vector spherical wave functions, without taking the complex conjugate of their radial parts, i.e., $\bar{\mathbf{F}}_{Hlm}(q,\mathbf{r}) = f_l(qr)\mathbf{X}^{\star}_{lm}(\mathbf{r})$, $\bar{\mathbf{F}}_{Elm}(q,\mathbf{r}) = -\frac{i}{q}\nabla \times f_l(qr)\mathbf{X}^{\star}_{lm}(\mathbf{r})$, for any kind of vector spherical wave functions $\mathbf{F} = \mathbf{J}$ or $\mathbf{H}$ (correspondingly $f_l = j_l$ or h_l^+).

We now apply the vector Green's theorem for a regular surface S_1 bounding a volume V_1,

$$\int_{V_1} \mathrm{d}^3 r \left[\mathbf{a}\cdot(\nabla\times\nabla\times\mathbf{b}) - (\nabla\times\nabla\times\mathbf{a})\cdot\mathbf{b}\right]$$

$$= -\int_{S_1} \mathrm{d}^2 r \left[\hat{\mathbf{n}}\times(\nabla\times\mathbf{a})\cdot\mathbf{b} + (\hat{\mathbf{n}}\times\mathbf{a})\cdot(\nabla\times\mathbf{b})\right], \quad \textbf{(12)}$$

where $\hat{\mathbf{n}}$ is the unit vector along the local outward normal to the surface, to the exterior region, inserting $\mathbf{a} = \mathbf{E}^{(n)}_{\mathrm{out}}(\mathbf{r})$ and $\mathbf{b} = \overleftrightarrow{G}(\mathbf{r},\mathbf{r}';\omega_n)\cdot\mathbf{c}$, where $\mathbf{c}$ is an arbitrary constant vector. The surface integral on the r.h.s. of Eq. (12) is the sum of two integrals: an integral over the spherical surface S_∞ bounding the exterior region at infinity and an integral over the surface of the object. With the help of Eqs. (9) and (10), Eq. (12) yields

$$\left[-\int_{S_\infty}\mathrm{d}^2 r + \int_S \mathrm{d}^2 r\right]\left[\left[\hat{\mathbf{n}}\times\left[\nabla\times\mathbf{E}^{(n)}_{\mathrm{out}}(\mathbf{r})\right]\right]\cdot\left[\overleftrightarrow{G}(\mathbf{r},\mathbf{r}';\omega_n)\cdot\mathbf{c}\right]\right.$$

$$\left.+\left[\hat{\mathbf{n}}\times\mathbf{E}^{(n)}_{\mathrm{out}}(\mathbf{r})\right]\cdot\left[\nabla\times\overleftrightarrow{G}(\mathbf{r},\mathbf{r}';\omega_n)\cdot\mathbf{c}\right]\right]$$

$$= \begin{cases} \mathbf{E}^{(n)}_{\mathrm{out}}(\mathbf{r}')\cdot\mathbf{c}, & \text{if } \mathbf{r}'\in V_{\mathrm{out}} \\ 0, & \text{if } \mathbf{r}'\in V_{\mathrm{in}}, \end{cases} \quad \textbf{(13)}$$

where $\hat{\mathbf{n}}$ is the local normal at either S_∞ or S and is directed away from the object. Since $\mathbf{c}$ is arbitrary, it can be canceled out on both sides of Eq. (13). Because the scattered field vanishes at infinity, in the integral over S_∞, we can substitute $\mathbf{E}^{(n)}_{\mathrm{out}}(\mathbf{r})$ by $\mathbf{E}^{(n)}_{\mathrm{inc}}(\mathbf{r})$. Then, applying Eq. (12) in all space for $\mathbf{a} = \mathbf{E}^{(n)}_{\mathrm{inc}}(\mathbf{r})$ and $\mathbf{b} = \overleftrightarrow{G}(\mathbf{r},\mathbf{r}';\omega_n)$, we obtain

$$\mathbf{E}^{(n)}_{\mathrm{inc}}(\mathbf{r}') = -\int_{S_\infty}\mathrm{d}^2 r\left[\left[\hat{\mathbf{n}}\times\left[\nabla\times\mathbf{E}^{(n)}_{\mathrm{inc}}(\mathbf{r})\right]\right]\cdot\overleftrightarrow{G}(\mathbf{r},\mathbf{r}';\omega_n)\right.$$

$$\left.+\left[\hat{\mathbf{n}}\times\mathbf{E}^{(n)}_{\mathrm{inc}}(\mathbf{r})\right]\cdot\left[\nabla\times\overleftrightarrow{G}(\mathbf{r},\mathbf{r}';\omega_n)\right]\right]. \quad \textbf{(14)}$$

Thus, Eq. (13) leads to

$$\mathbf{E}^{(n)}_{\mathrm{inc}}(\mathbf{r}') + \int_S \mathrm{d}^2 r\left[i\omega_n\mu_0\mu\left[\hat{\mathbf{n}}\times\mathbf{H}^{(n)}_{\mathrm{out}}(\mathbf{r})\right]\cdot\overleftrightarrow{G}(\mathbf{r},\mathbf{r}';\omega_n)\right.$$

$$\left.+\left[\hat{\mathbf{n}}\times\mathbf{E}^{(n)}_{\mathrm{out}}(\mathbf{r})\right]\cdot\left[\nabla\times\overleftrightarrow{G}(\mathbf{r},\mathbf{r}';\omega_n)\right]\right]$$

$$= \begin{cases} \mathbf{E}^{(n)}_{\mathrm{out}}(\mathbf{r}'), & \text{if } \mathbf{r}'\in V_{\mathrm{out}} \\ 0, & \text{if } \mathbf{r}'\in V_{\mathrm{in}}\,. \end{cases} \quad \textbf{(15)}$$

From the continuity of the tangential components of the EM field at the surface of the object at any moment in time, we obtain $\hat{\mathbf{n}}\times\mathbf{H}^{(n)}_{\mathrm{out}}(\mathbf{r}) = \hat{\mathbf{n}}\times\mathbf{H}^{(n)}_{\mathrm{in}}(\mathbf{r})$ and $\hat{\mathbf{n}}\times\mathbf{E}^{(n)}_{\mathrm{out}}(\mathbf{r}) = \hat{\mathbf{n}}\times\mathbf{E}^{(n)}_{\mathrm{in}}(\mathbf{r})$. Using Eq. (11) and the vector identity $(\mathbf{a}\times\mathbf{b})\cdot\mathbf{c} = \mathbf{a}\cdot(\mathbf{b}\times\mathbf{c})$, Eq. (15) yields

$$\mathbf{E}^{(n)}_{\mathrm{sc}}(\mathbf{r}') = iq_{\mathrm{h}n}\sum_L \mathbf{H}_L(q_{\mathrm{h}n},\mathbf{r}')\int_S \mathrm{d}^2 r\,\hat{\mathbf{n}}\cdot\left[\frac{\mu_{\mathrm{h}}}{\mu}\left[\nabla\times\mathbf{E}^{(n)}_{\mathrm{in}}(\mathbf{r})\right]\right.$$

$$\left.\times\bar{\mathbf{J}}_L(q_{\mathrm{h}n},\mathbf{r}) + \mathbf{E}^{(n)}_{\mathrm{in}}(\mathbf{r})\times\left[\nabla\times\bar{\mathbf{J}}_L(q_{\mathrm{h}n},\mathbf{r})\right]\right], \quad \mathbf{r}'\in V_{\mathrm{out}} \quad \textbf{(16)}$$

and

$$\mathbf{E}^{(n)}_{\mathrm{inc}}(\mathbf{r}') = -iq_{\mathrm{h}n}\sum_L \mathbf{J}_L(q_{\mathrm{h}n},\mathbf{r}')\int_S \mathrm{d}^2 r\,\hat{\mathbf{n}}\cdot\left[\frac{\mu_{\mathrm{h}}}{\mu}\left[\nabla\times\mathbf{E}^{(n)}_{\mathrm{in}}(\mathbf{r})\right]\right.$$

$$\left.\times\bar{\mathbf{H}}_L(q_{\mathrm{h}n},\mathbf{r}) + \mathbf{E}^{(n)}_{\mathrm{in}}(\mathbf{r})\times\left[\nabla\times\bar{\mathbf{H}}_L(q_{\mathrm{h}n},\mathbf{r})\right]\right], \quad \mathbf{r}'\in V_{\mathrm{in}}. \quad \textbf{(17)}$$

Comparing Eqs. (16) and (17) with Eqs. (6) and (4), respectively, we obtain

$$a_L^{+(n)} = \sum_{L'\nu} Q^{+}_{Ln;L'\nu}a_{L'\nu},$$

$$a_L^{0(n)} = -\sum_{L'\nu} Q^{0}_{Ln;L'\nu}a_{L'\nu}, \quad \textbf{(18)}$$

where

$$Q^{+}_{Ln;L'\nu} = iq_{\mathrm{h}n}v_{n;\nu}\int_S \mathrm{d}^2 r\,\hat{\mathbf{n}}\cdot\left[\mathbf{J}_{L'}(q_\nu,\mathbf{r})\times\left[\nabla\times\bar{\mathbf{J}}_L(q_{\mathrm{h}n},\mathbf{r})\right]\right.$$

$$\left.-\frac{\mu_{\mathrm{h}}}{\mu}\bar{\mathbf{J}}_L(q_{\mathrm{h}n},\mathbf{r})\times\left[\nabla\times\mathbf{J}_{L'}(q_\nu,\mathbf{r})\right]\right] \quad \textbf{(19)}$$

and

$$Q^{0}_{Ln;L'\nu} = iq_{\mathrm{h}n}v_{n;\nu}\int_S \mathrm{d}^2 r\,\hat{\mathbf{n}}\cdot\left[\mathbf{J}_{L'}(q_\nu,\mathbf{r})\times\left[\nabla\times\bar{\mathbf{H}}_L(q_{\mathrm{h}n},\mathbf{r})\right]\right.$$

$$\left.-\frac{\mu_{\mathrm{h}}}{\mu}\bar{\mathbf{H}}_L(q_{\mathrm{h}n},\mathbf{r})\times\left[\nabla\times\mathbf{J}_{L'}(q_\nu,\mathbf{r})\right]\right]. \quad \textbf{(20)}$$

From Eq. (18) and the general definition of the T matrix, $a_L^{+(n)} = \sum_{L'n'} T_{Ln;L'n'}a_{L'}^{0(n')}$, we obtain

$$\sum_{L''n''} T_{Ln;L''n''}\,Q^{0}_{L''n'';L'\nu} = -Q^{+}_{Ln;L'\nu}. \quad \textbf{(21)}$$

Obviously, in the absence of any modulation, the $Q^{+(0)}$ matrices become diagonal in $n\nu$ because $v_{n;\nu}$ is diagonal, and we recover the result of the unmodulated case [12].

Although the spherical-wave expansions of the EM field are infinite series, it turns out that, if the size of the scatterer is not much larger than the wavelength, a limited number of partial waves, up to a maximum angular momentum $l_{\max}$, is sufficient to describe the scattered field using the T matrix. However,

to accurately evaluate the elements of the T matrix of given dimensions, matrices of larger size must be considered in the linear system of Eq. (21), which is solved, e.g., by Gaussian elimination. This implies that we keep matrix elements up to cutoff values $l_{\rm cut} \geq l_{\rm max}$ and $N_{\rm cut} \geq N$. Obviously, for spherical particles, $l_{\rm cut} = l_{\rm max}$, but $l_{\rm cut}$ should be increased as the shape of the scatterer deviates from the sphere while N and $N_{\rm cut}$ depend on the characteristics of the periodic modulation. While there are no established guidelines for determining the suitable parameters to ensure the convergence of the series expansions, a comprehensive examination of the convergence characteristics of the EBCM is available in [4]. In the applications presented in the next section, choosing $l_{\rm max} = 8$, $l_{\rm cut} = 12$ and $N = 3$, $N_{\rm cut} = 6$, we obtained convergence within seven digits in all results.

Taking advantage of the general relations $\nabla \times \mathbf{F}_{Hlm}(q, \mathbf{r}) = -iq\mathbf{F}_{Elm}(q, \mathbf{r})$, $\nabla \times \mathbf{F}_{Elm}(q, \mathbf{r}) = iq\mathbf{F}_{Hlm}(q, \mathbf{r})$ and $\nabla \times \bar{\mathbf{F}}_{Hlm}(q, \mathbf{r}) = iq\bar{\mathbf{F}}_{Elm}(q, \mathbf{r})$, $\nabla \times \bar{\mathbf{F}}_{Elm}(q, \mathbf{r}) = -iq\bar{\mathbf{F}}_{Hlm}(q, \mathbf{r})$ between any kind ($\mathbf{F} = \mathbf{J}$ or $\mathbf{H}$) of vector spherical wave functions, Eqs. (19) and (20) can be written in the following form:

$$
\begin{aligned}
Q^{+(0)}_{Hlmn;\,Hl'm'\nu} &= -\frac{q_{{\rm h}n}}{q_\nu}\mathcal{J}^{+(0)}_{Elmn;\,Hl'm'\nu} + \frac{\mu_{\rm h}}{\mu}\mathcal{J}^{+(0)}_{Hlmn;\,El'm'\nu}\,,\\
Q^{+(0)}_{Hlmn;\,El'm'\nu} &= -\frac{q_{{\rm h}n}}{q_\nu}\mathcal{J}^{+(0)}_{Elmn;\,El'm'\nu} - \frac{\mu_{\rm h}}{\mu}\mathcal{J}^{+(0)}_{Hlmn;\,Hl'm'\nu}\,,\\
Q^{+(0)}_{Elmn;\,El'm'\nu} &= \frac{q_{{\rm h}n}}{q_\nu}\mathcal{J}^{+(0)}_{Hlmn;\,El'm'\nu} - \frac{\mu_{\rm h}}{\mu}\mathcal{J}^{+(0)}_{Elmn;\,Hl'm'\nu}\,,\\
Q^{+(0)}_{Elmn;\,Hl'm'\nu} &= \frac{q_{{\rm h}n}}{q_\nu}\mathcal{J}^{+(0)}_{Hlmn;\,Hl'm'\nu} + \frac{\mu_{\rm h}}{\mu}\mathcal{J}^{+(0)}_{Elmn;\,El'm'\nu},
\end{aligned}
\tag{22}
$$

with the help of the following simple surface integrals of cross products of vector spherical wave functions,

$$
\begin{aligned}
\mathcal{J}^{+}_{Ln;\,L'\nu} &= q_{{\rm h}n}q_\nu \upsilon_{n;\nu}\int_S {\rm d}^2 r\,\hat{\mathbf{n}}\cdot\left[\mathbf{J}_{L'}(q_\nu,\mathbf{r})\times\bar{\mathbf{J}}_L(q_{{\rm h}n},\mathbf{r})\right],\\
\mathcal{J}^{0}_{Ln;\,L'\nu} &= q_{{\rm h}n}q_\nu \upsilon_{n;\nu}\int_S {\rm d}^2 r\,\hat{\mathbf{n}}\cdot\left[\mathbf{J}_{L'}(q_\nu,\mathbf{r})\times\bar{\mathbf{H}}_L(q_{{\rm h}n},\mathbf{r})\right].
\end{aligned}
\tag{23}
$$

In spherical coordinates, the points at the surface of the object are defined by a position vector $\mathbf{r}(\theta,\phi) = r(\theta,\phi)\hat{\mathbf{r}}$, which depends on the polar and azimuthal angles, θ and ϕ, respectively, and the surface integrals in Eqs. (23) can be evaluated by substituting

$$
d^2 r\,\hat{\mathbf{n}} = \left(r^2\sin\theta\,\hat{\mathbf{r}} - r\sin\theta\frac{\partial r}{\partial\theta}\hat{\boldsymbol{\theta}} - r\frac{\partial r}{\partial\phi}\hat{\boldsymbol{\phi}}\right)d\theta\,d\phi \tag{24}
$$

and using numerical quadrature integration [4]. For bodies of revolution—which possess azimuthal symmetry, $\mathbf{r}(\theta,\phi) = r(\theta)\hat{\mathbf{r}}$, and/or, in addition, cylindrical symmetry, $r(\pi-\theta) = r(\theta)$—the ϕ-integration can be carried out analytically, and closed-form expressions for the remaining polar integrals can be found elsewhere [4,12]. These integrals must be evaluated numerically. In the applications presented in the next section for spheroidal particles, using a Gaussian quadrature integration formula with 64 points, we obtained converged results within seven digits.

In the special case of a spherical body, $\mathbf{r}(\theta,\phi) = R\hat{\mathbf{r}}$, and Eqs. (23) yield

$$
\begin{aligned}
&\mathcal{J}^{+(0)}_{Hlmn;\,Hl'm'\nu} = 0,\ \mathcal{J}^{+(0)}_{Elmn;\,El'm'\nu} = 0\,,\\
&\mathcal{J}^{+}_{Elmn;\,Hl'm'\nu} = -ix_n x_\nu \upsilon_{n;\nu} j_l(x_\nu)\frac{[x_n j_l(x_n)]'}{x_n}\delta_{ll'}\delta_{mm'}\,,\\
&\mathcal{J}^{+}_{Hlmn;\,El'm'\nu} = -ix_n x_\nu \upsilon_{n;\nu} j_l(x_n)\frac{[x_\nu j_l(x_\nu)]'}{x_\nu}\delta_{ll'}\delta_{mm'}\,,\\
&\mathcal{J}^{0}_{Elmn;\,Hl'm'\nu} = -ix_n x_\nu \upsilon_{n;\nu} j_l(x_\nu)\frac{[x_n h^+_l(x_n)]'}{x_n}\delta_{ll'}\delta_{mm'}\,,\\
&\mathcal{J}^{0}_{Hlmn;\,El'm'\nu} = -ix_n x_\nu \upsilon_{n;\nu} h^+_l(x_n)\frac{[x_\nu j_l(x_\nu)]'}{x_\nu}\delta_{ll'}\delta_{mm'},
\end{aligned}
\tag{25}
$$

where $x_n \equiv q_{{\rm h}n}R$, $x_\nu \equiv q_\nu R$ and the prime denotes the derivative of a function with respect to the only variable upon which it depends. Using Eqs. (25), it can be shown that Eq. (21) yields a T matrix diagonal in Plm, and independent of m, and the linear system of Eq. (21) becomes equivalent to that obtained by directly imposing the boundary conditions at the surface of the sphere [37,40,41]. This validates the correctness of the generalized EBCM for periodically time-modulated scatterers of arbitrary shape, presented here.

3. RESULTS AND DISCUSSION

We shall now demonstrate the applicability of the method developed in the previous section on plane wave scattering by a periodically driven dielectric body of revolution with its symmetry axis, say, along the z direction.

The electric field associated with a single monochromatic plane EM wave, of angular frequency ω, $\mathbf{E}_0(\mathbf{r},t) = {\rm Re}[\mathbf{E}_0(\mathbf{r})\exp(-i\omega t)]$, propagating in the host medium with wave vector $\mathbf{q}_{\rm h} = \hat{\mathbf{q}}_{\rm h}\omega\sqrt{\epsilon_{\rm h}\mu_{\rm h}}/c$, has the form $\mathbf{E}_0(\mathbf{r}) = \hat{\mathbf{p}}E_0\exp(i\mathbf{q}_{\rm h}\cdot\mathbf{r})$, where E_0 is the magnitude and $\hat{\mathbf{p}}$, a unit vector, denotes the polarization of the wave. Writing the amplitudes in an expansion into partial spherical waves, similar to that of Eq. (4), as

$$
a^0_{Plm} = \mathbf{A}^0_{Plm}(\hat{\mathbf{q}}_{\rm h})\cdot\hat{\mathbf{p}}E_0\,, \tag{26}
$$

one can derive explicit expressions for the vector coefficients $\mathbf{A}^0_{Plm}$ in terms of the usual spherical harmonics Y^m_l, which are functions of the angular variables (θ,ϕ) of $\hat{\mathbf{q}}_{\rm h}$ in the chosen system of spherical coordinates. We obtain

$$
\begin{aligned}
\mathbf{A}^0_{Elm}(\hat{\mathbf{q}}_{\rm h}) = C_{lm}\Big[&i\left[\alpha^m_l e^{i\phi}Y^{-m-1}_l(\theta,\phi) - \alpha^{-m}_l e^{-i\phi}Y^{-m+1}_l(\theta,\phi)\right]\hat{\mathbf{e}}_\theta\\
&-\left[\alpha^m_l\cos\theta\,e^{i\phi}Y^{-m-1}_l(\theta,\phi) + m\sin\theta\,Y^{-m}_l(\theta,\phi)\right.\\
&\left.+\,\alpha^{-m}_l\cos\theta\,e^{-i\phi}Y^{-m+1}_l(\theta,\phi)\right]\hat{\mathbf{e}}_\phi\Big]
\end{aligned}
\tag{27}
$$

and

$$\mathbf{A}^0_{Hlm}(\hat{\mathbf{q}}_\mathrm{h}) = C_{lm}\Big[\big[\alpha_l^m \cos\theta e^{i\phi} Y_l^{-m-1}(\theta,\phi) + m\sin\theta Y_l^{-m}(\theta,\phi) + \alpha_l^{-m}\cos\theta e^{-i\phi} Y_l^{-m+1}(\theta,\phi)\big]\hat{\mathbf{e}}_\theta + i\big[\alpha_l^m e^{i\phi} Y_l^{-m-1}(\theta,\phi) - \alpha_l^{-m} e^{-i\phi} Y_l^{-m+1}(\theta,\phi)\big]\hat{\mathbf{e}}_\phi\Big], \tag{28}$$

where $C_{lm} = 4\pi i^l (-1)^{m+1}/\sqrt{l(l+1)}$, $\alpha_l^m = \sqrt{(l-m)(l+m+1)}/2$, and $\hat{\mathbf{e}}_\theta, \hat{\mathbf{e}}_\phi$ are the polar and azimuthal unit vectors, respectively, which are perpendicular to $\hat{\mathbf{q}}_\mathrm{h}$.

We define the (normalized) scattering cross section as the ratio of the energy flux scattered by the body to the incident energy flux through the maximum geometric cross section of a sphere of equal volume, i.e., a circle of area πR^2, where R is the sphere radius. After some straightforward algebra, we obtain

$$\sigma_\mathrm{sc} = \sum_n \frac{1}{\pi (q_{\mathrm{h}n} R)^2} \sum_L \left| \sum_{L'} T_{Ln;L'0} \mathbf{A}^0_{L'}(\hat{\mathbf{q}}_\mathrm{h}) \cdot \hat{\mathbf{p}} \right|^2 \equiv \sum_n \sigma_\mathrm{sc}^{(n)}, \tag{29}$$

where $\sigma_\mathrm{sc}^{(n)}$ should be interpreted as the cross section associated with the nth order inelastic scattering, which yields beams with angular frequency $\omega - n\Omega$. In the particular case of a spherical scatterer, the T matrix becomes diagonal, $T_{Plmn;P'l'm'0} = T_{Pl}^{n0} \delta_{PP'} \delta_{ll'} \delta_{mm'}$. By taking advantage of the identity $\sum_m |\mathbf{A}^0_{Plm}(\hat{\mathbf{q}}_\mathrm{h}) \cdot \hat{\mathbf{p}}|^2 = 2\pi(2l+1)$, we recover the result for the scattering cross section of a periodically driven sphere [37]. It is clear from Eq. (29) that, contrary to a spherical scatterer, the cross section depends, in general, on the polarization, $\hat{\mathbf{p}}$, and the propagation direction, $\hat{\mathbf{q}}_\mathrm{h}$, of the incident wave. It is also worth noting that, for an unmodulated scatterer, the sum over n in Eq. (29) reduces to the single term for $n = 0$, and we recover the result for the (elastic) scattering cross section of a static object of arbitrary shape [12]. Correspondingly, the extinction cross section takes the following form:

$$\sigma_\mathrm{ext} = -\frac{1}{\pi (q_\mathrm{h} R)^2} \mathrm{Re} \sum_L \left[\mathbf{A}^0_L(\hat{\mathbf{q}}_\mathrm{h}) \cdot \hat{\mathbf{p}}\right]^\star \sum_{L'} T_{L0;L'0} \mathbf{A}^0_{L'}(\hat{\mathbf{q}}_\mathrm{h}) \cdot \hat{\mathbf{p}}, \tag{30}$$

and the absorption cross section is defined by $\sigma_\mathrm{abs} = \sigma_\mathrm{ext} - \sigma_\mathrm{sc}$.

In dielectric particles of cylindrical symmetry, the $(2l+1)$ degeneracy of a Mie mode, implied by spherical geometry, is (partially) lifted because the symmetry is reduced from O(3) to $\mathrm{D}_{\infty\mathrm{h}}$ [45]. Projecting onto the irreducible representations of the $\mathrm{D}_{\infty\mathrm{h}}$ point group, as listed in Table 1, one obtains $|m| = 0, 1, \ldots, l$ distinct modes. For $m = 0$, these modes are nondegenerate and have the symmetry of the one-dimensional irreducible representations $A_{1\mathrm{g}}$ for a TM (electric) multipole of even order, $A_{1\mathrm{u}}$ for a TE (magnetic) multipole of even order, $A_{2\mathrm{g}}$ for a TE (magnetic) multipole of odd order, and $A_{2\mathrm{u}}$ for a TM (electric) multipole of odd order. For $m \neq 0$, the modes are doubly degenerate and have the $E_{|m|\mathrm{g}}$ symmetry for a TM multipole of even order or a TE multipole of odd order, and the $E_{|m|\mathrm{u}}$ symmetry for a TM multipole of odd order or a TE multipole of even order [46]. This means that each $|m|$-split mode is characterized by a well-defined value of $|m|$ and parity (namely that of its degenerate parent Mie mode of the sphere). It has neither a specific polarization nor a specific multipole order in the strict sense though its dominant character is that of the parent Mie mode.

Table 1. Character Table of the $\mathrm{D}_{\infty\mathrm{h}}$ Point Group[a]

$\mathrm{D}_{\infty\mathrm{h}}$	E	$2C_\phi$	$C_{2'}$	I	$2IC_\phi$	$IC_{2'}$
$A_{1\mathrm{g}}$	1	1	1	1	1	1
$A_{1\mathrm{u}}$	1	1	1	−1	−1	−1
$A_{2\mathrm{g}}$	1	1	−1	1	1	−1
$A_{2\mathrm{u}}$	1	1	−1	−1	−1	1
$E_{\lvert m\rvert\mathrm{g}}$	2	$2\cos(\lvert m\rvert\phi)$	0	2	$2\cos(\lvert m\rvert\phi)$	0
$E_{\lvert m\rvert\mathrm{u}}$	2	$2\cos(\lvert m\rvert\phi)$	0	−2	$-2\cos(\lvert m\rvert\phi)$	0

[a] $|m| = 1, 2, 3, \ldots$. Here, C_ϕ represents rotation operations through an angle ϕ ($0 < \phi \leq \pi$ and $-\pi < \phi < 0$) about the symmetry axis (z), $C_{2'}$ are rotations through π about axes lying in the x–y plane, and I is the inversion operation.

In general, the change of the number of states of the EM field up to angular frequency ω, induced by a single particle in a host medium, can be evaluated with the help of the corersponding T matrix from

$$\Delta N(\omega) = \frac{1}{\pi} \mathrm{Im} \ln \det[\mathbf{I} + \mathbf{T}], \tag{31}$$

where $\mathbf{I}$ is the unit matrix [47]. Of more interest is the associated change of the density of states, $\Delta n(\omega) = d\Delta N(\omega)/d\omega$.

To discuss such properties at an actual example, let us begin with the static case, i.e., without time modulation, and consider a spheroidal germanium particle with semiaxes a and b, in air; a is the equatorial radius, and b is the distance from center to pole along the axis of revolution, z, of the spheroid. Figure 1 depicts the change of the density of states of the EM field, induced by the particle, in a frequency region about the corresponding $\mathrm{TM}_{l=3}$ (electric octupole) and $\mathrm{TE}_{l=4}$ (magnetic hexadecapole) Mie modes, by varying the aspect ratio $\beta = b/a$. The degeneracy lifting ($|m|$-mode splitting) due to deviation from sphericity is clearly visible in the figure. Since we shall be interested in a relatively restricted spectral range at the infrared

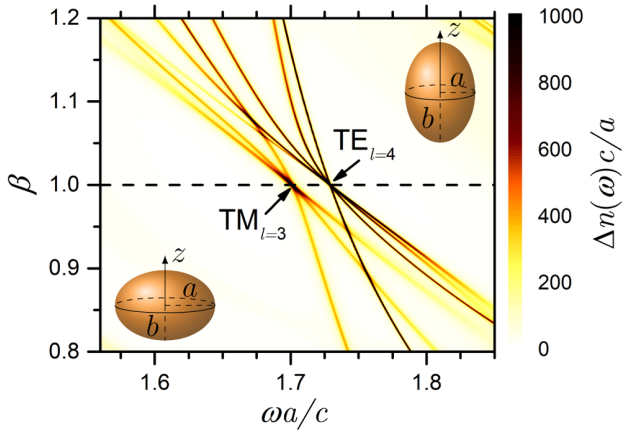

Fig. 1. Change of the density of states of the EM field, due to a spheroidal germanium particle ($\epsilon = 16, \mu = 1$) with aspect ratio β, in air, in a spectral region about the $\mathrm{TM}_{l=3}$ and $\mathrm{TE}_{l=4}$ Mie modes. The dashed horizontal line corresponds to the sphere shape. The system is assumed to be static, i.e., with no time modulation.

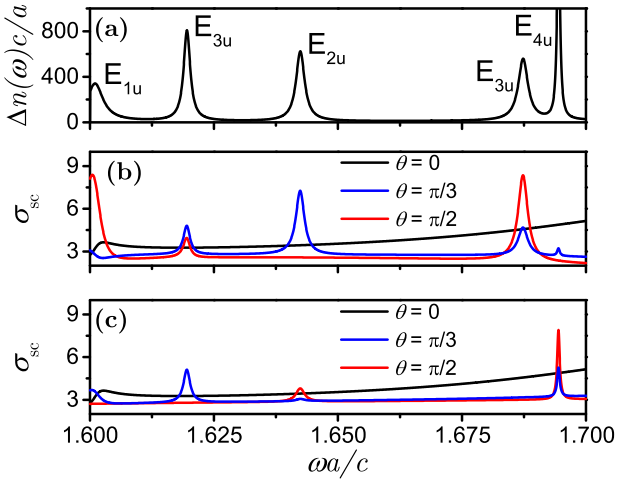

Fig. 2. (a) Change of the density of states of the EM field, due to a prolate spheroidal germanium particle ($\epsilon = 16$, $\mu = 1$) with aspect ratio $\beta = 1.2$, in air, within a restricted frequency range in the vicinity of the $TM_{l=3}$ and $TE_{l=4}$ Mie modes. (b) and (c) Corresponding scattering cross section, for light incident at an angle $\theta = 0, \pi/3$, and $\pi/2$ with respect to the revolution axis of the particle, polarized along $\hat{\mathbf{e}}_\phi$ and $\hat{\mathbf{e}}_\theta$, respectivly. Again, the system is assumed to be static, i.e., with no time modulation.

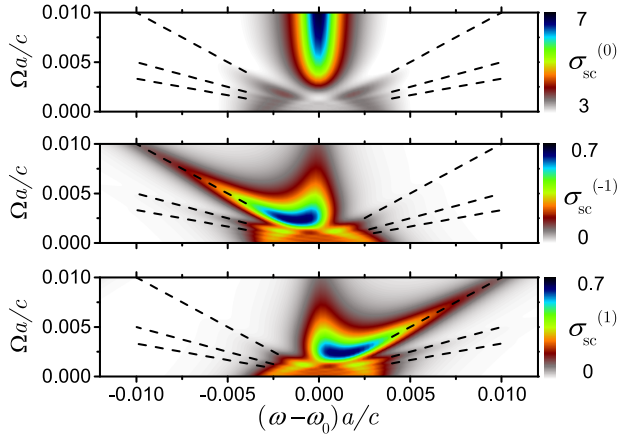

Fig. 3. Elastic and first-order inelastic optical scattering cross sections of a time-modulated prolate sheroidal germanium particle ($\mu = 1$, $\epsilon(t) = 16[1 + 0.004\cos(\Omega t)]$) with aspect ratio $\beta = 1.2$, in air, for light of angular frequency ω incident at an angle $\theta = \pi/3$ with respect to the revolution axis of the particle and polarized along $\hat{\mathbf{e}}_\phi$, about the E_{2u} resonant mode of the unmodulated particle (see Fig. 2), at ω_0, by varying the modulation frequency. The straight dashed lines express the conditions $\omega - \omega_0 = n\Omega$, $n = \pm 1, \pm 2, \pm 3$.

part of the spectrum where germanium can be assumed dispersionless with a constant relative electric permittivity $\epsilon = 16$ and magnetic permeability $\mu = 1$, our results remain the same at different frequencies, provided that the size of the particle is scaled accordingly. For this reason, we represent the results as a function of the dimensionless frequency $\omega a/c$.

We shall next focus our study on the optical states of a germanium prolate spheroidal particle, with aspect ratio $\beta = 1.2$, which originate from the $TM_{l=3}$ and $TE_{l=4}$ Mie modes, within a restricted frequency range from $\omega a/c = 1.6$ to $\omega a/c = 1.7$ [see Fig. 2(a)]. These states are manifested differently in the scattering cross section of an incident plane EM wave, depending on the polarization, $\hat{\mathbf{p}}$, and the propagation direction, $\hat{\mathbf{q}}_h$, of the incident wave, according to Eq. (29). More specifically, concerning the odd parity (u) modes that are relevant in the case under consideration, a plane wave incident along the revolution axis of the particle ($\theta = 0, \pi$), at any polarization, couples only with the E_{1u} modes while, if incident at any angle $\theta \neq 0, \pi/2, \pi$, it couples with all $E_{|m|u}$ and with either the A_{1u} or the A_{2u} modes, if $\hat{\mathbf{p}} = \hat{\mathbf{e}}_\phi$ or $\hat{\mathbf{p}} = \hat{\mathbf{e}}_\theta$, respectively. In the particular case of an incidence normal to the revolution axis ($\theta = \pi/2$), $A_{1u}, E_{2u}, E_{4u}, \ldots$ modes are not excited if $\hat{\mathbf{p}} = \hat{\mathbf{e}}_\phi$, while $E_{1u}, E_{3u}, \ldots$ modes are not excited if $\hat{\mathbf{p}} = \hat{\mathbf{e}}_\theta$ [46]. This selective excitation of the particle modes is clearly visible in Figs. 2(b) and 2(c). However, it should be noted that an incident wave couples to a different degree with a non-symmetry-forbidden particle mode, depending on its polarization and propagation direction. For example, a wave incident at an angle $\theta = \pi/3$ with respect to the particle's axis of revolution and polarization direction $\hat{\mathbf{p}} = \hat{\mathbf{e}}_\theta$ couples very weakly with the E_{2u} mode and the E_{3u} mode at $\omega a/c = 1.687$ shown in Fig. 2(a), as we can infer from Fig. 2(c), where the corresponding peaks in the scattering cross section are not discernible.

We will now investigate the effect of a periodic modulation of the electric permittivity, of the following form:

$$\epsilon(t) = \epsilon[1 + \eta\cos(\Omega t)], \tag{32}$$

where $\epsilon = 16$ is the static relative electric permittivity of the germanium particle, while η and Ω are the relative amplitude and angular frequency of the modulation, respectively. In terms of experimental implementation, alongside electro-optical modulation capable of reaching frequencies on the order of tens of gigahertz in common semiconductor materials [48], it is possible to achieve strong, ultrafast periodic modulation through the optical stimulation of free carriers using femtosecond pump laser pulses [49,50].

As a rule, strong elastic scattering is encountered when a resonant mode is excited, while increased inelastic scattering is also expected when the final photon state is at a resonance mode, i.e., when the detuning of the incident wave frequency from a particle resonance equals an integer multiple of Ω.

We depict in Fig. 3 the cross sections associated with the elastic (Rayleigh, $n = 0$) and first-order inelastic (anti-Stokes, $n = -1$ and Stokes, $n = 1$) scattering, about the E_{2u} mode shown in Fig. 2, versus the modulation frequency, for a rather moderate amplitude $\eta = 0.004$. It can be seen that, when the modulation is switched on, Rayleigh scattering at resonance is reduced and the intensity is transferred to the inelastically scattered beams. Since the inelastic scattering depends, also, on the final photon state, by increasing Ω beyond the resonance width, a gradual reduction of inelastic scattering at resonance is encountered. In contrast, the corresponding Rayleigh component grows back to its value in the unmodulated case. Therefore, as the modulation frequency becomes higher, time variation does not affect considerably the scattering cross sections at resonance because the density of optical states drastically decreases outside the resonance. On the other hand, if the frequency of

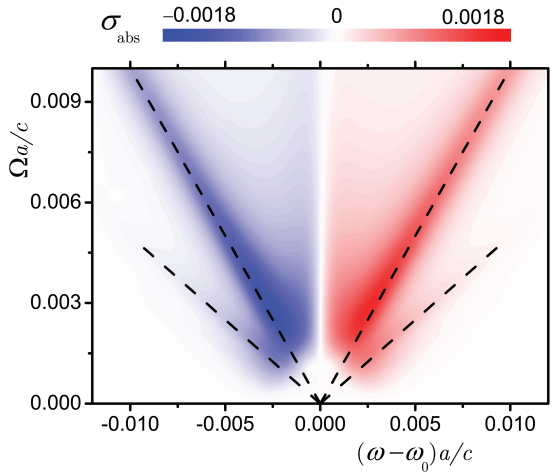

Fig. 4. Absorption cross section of a time-modulated prolate sheroidal germanium particle ($\mu = 1$, $\epsilon(t) = 16[1 + 0.004\cos(\Omega t)]$) with aspect ratio $\beta = 1.2$, in air, for light of angular frequency ω incident at an angle $\theta = \pi/3$ with respect to the revolution axis of the particle and polarized along $\hat{\mathbf{e}}_\phi$, about the E_{2u} resonant mode of the unmodulated particle (see Fig. 2), at ω_0, by varying the modulation frequency. The straight dashed lines express the conditions of resonant inelastic scattering, $\omega - \omega_0 = \pm\Omega, \pm 2\Omega$.

the incident wave is off-resonance, elastic and inelastic scattering is generally weak, except when detuning from resonance matches an integer multiple of the modulation frequency. In this case, inelastic scattering processes involving upconverted or downconverted photons by the proper number of frequency quanta Ω are favored. Figure 3 shows how all relevant states of the EM field, at $\omega = \omega_0 - n\Omega$, $n = 0, \pm 1, \pm 2, \ldots$, coupled through the periodic modulation, manifest themselves in the Rayleigh and first-order anti-Stokes and Stokes scattering cross-section channels. By increasing the modulation amplitude, higher-order inelastic scattering processes become more prominent.

It should be pointed out that, in a dynamical system, even in the absence of intrinsic losses as considered in the present work, we may have an exchange of energy between the modulation and the EM field. This is clearly manifested in Fig. 4, especially when the conditions for resonant inelastic scattering are fulfilled. Specifically, for the anti-Stokes beams with upconverted frequency $\omega + n\Omega$, $n > 0$, where the photons absorb n frequency quanta Ω, the EM field gains energy, which is manifested as a negative absorption cross section. Correspondingly, for the Stokes beams, where the photons emit n frequency quanta Ω, we have energy loss, i.e., a positive absorption cross section. It can be seen that, at low values of Ω where the adiabatic description is valid, the energy of the EM field is conserved. This is also the case for an incidence about the resonance frequency. In that case, frequency upconversion and downconversion processes have more or less equal weight, and the associated energy gain and loss mechanisms counterbalance each other.

Quite importantly, the effects discussed above, which result from resonant inelastic scattering by a nonspherical particle, critically depend on the polarization and the propagation direction of the incident wave. For example, by switching the polarization direction from $\hat{\mathbf{p}} = \hat{\mathbf{e}}_\phi$ to $\hat{\mathbf{p}} = \hat{\mathbf{e}}_\theta$, the E_{2u} mode is inactivated due to inefficient coupling (see Fig. 2), and we obtain corresponding featureless, weak scattering patterns, as opposed to those depicted in Figs. 3 and 4. Therefore, nonspherical scatterers allow one to tailor spectral resonances at will and control consequent effects by external means.

4. CONCLUSION

In summary, we extended the EBCM to describe EM scattering from a homogeneous and isotropic body of arbitrary shape, characterized by an electric permittivity that varies periodically in time. The corresponding scattering T matrix is calculated by numerically solving a linear system of algebraic equations similar to, but of greater dimensions than, that in the static case, which reduces analytically to the results obtained in the literature for the unmodulated nonspherical scatterer and the modulated sphere in the proper limits, i.e., in the absence of modulation and for a spherical shape, respectively.

We demonstrated the applicability of the method on a specific example of a periodically driven spheroidal germanium particle and revealed the occurrence of strong, resonant inelastic light scattering accompanied by energy transfer between the scatterer and the EM field, when the detuning of the incident wave frequency from a particle resonance matches an integer multiple of the modulation frequency. More importantly, we provided compelling evidence that nonspherical scatterers allow one to tailor spectral resonances at will and control consequent effects by external means, such as the polarization and the propagation direction of the incident light beam. We provided a consistent interpretation of the underlying physics and highlighted the role of symmetry based on a group theory analysis.

The generalized EBCM reported in the present work can be readily implemented into the recently developed dynamic versions of multiple-scattering computational methodologies. Owing to the controllable accuracy, computational efficiency, and facile implementation of the dynamic EBCM, exploration of wider classes of dynamic photonic structures, with temporally modulated building units of various shapes, will become within reach. Furthermore, the dynamic EBCM outlined in this paper has the potential for expansion to encompass anisotropic objects, such as gyrotropic bodies of revolution, in a manner akin to the approach taken by Zouros *et al*. [7]. It can also be applied to inhomogeneous objects composed of multiple homogeneous shells through the utilization of a recursive methodology [51–53].

Funding. Deutsche Forschungsgemeinschaft (Project-ID No. 258734477, SFB 1173).

Acknowledgment. P. G. and C. R. are part of the Max Planck School of Photonics, supported by the Bundesministerium für Bildung und Forschung, the Max Planck Society, and the Fraunhofer Society. P.G. acknowledges support from the Karlsruhe School of Optics and Photonics (KSOP). P. G. and C. R. acknowledge support by the German Research Foundation within the SFB 1173.

Disclosures. The authors declare no conflicts of interest.

Data Availability. The generating code used to produce the presented results is available from the corresponding author upon request.

REFERENCES

1. P. Waterman, "Matrix formulation of electromagnetic scattering," Proc. IEEE **53**, 805–812 (1965).
2. P. C. Waterman, "Symmetry, unitarity, and geometry in electromagnetic scattering," Phys. Rev. D **3**, 825–839 (1971).
3. P. Barber and C. Yeh, "Scattering of electromagnetic waves by arbitrarily shaped dielectric bodies," Appl. Opt. **14**, 2864–2872 (1975).
4. M. I. Mishchenko, L. D. Travis, and A. A. Lacis, *Scattering, Absorption, and Emission of Light by Small Particles* (Cambridge University, 2002).
5. M. I. Mishchenko, G. Videen, V. A. Babenko, N. G. Khlebtsov, and T. Wriedt, "T-matrix theory of electromagnetic scattering by particles and its applications: a comprehensive reference database," J. Quant. Spectrosc. Radiat. Transfer **88**, 357–406 (2004).
6. E. Almpanis, N. Papanikolaou, and N. Stefanou, "Nonspherical optomagnonic resonators for enhanced magnon-mediated optical transitions," Phys. Rev. B **104**, 214429 (2021).
7. G. P. Zouros, G. D. Kolezas, N. Stefanou, and T. Wriedt, "EBCM for electromagnetic modeling of gyrotropic BoRs," IEEE Trans. Anntenas Propag. **69**, 6134–6139 (2021).
8. G. P. Zouros, G. D. Kolezas, and K. Katsinos, "Em scattering by core-shell gyroelectric-isotropic and isotropic-gyroelectric BoRs using the EBCM," IEEE J. Multiscale Multiphys. Comput. Tech. **7**, 117–125 (2022).
9. D. W. Mackowski, "Chapter 6—T-matrix method for particles of arbitrary shape and composition," in *Light, Plasmonics and Particles (Nanophotonics)*, M. P. Menguc and M. Francoeur, eds. (Elsevier, 2023), pp. 113–131.
10. M. I. Mishchenko and L. D. Travis, "T-matrix computations of light scattering by large spheroidal particles," Opt. Commun. **109**, 16–21 (1994).
11. M. F. Iskander and A. Lakhtakia, "Extension of the iterative EBCM to calculate scattering by low-loss or lossless elongated dielectric objects," Appl. Opt. **23**, 948–953 (1984).
12. G. Gantzounis and N. Stefanou, "Layer-multiple-scattering method for photonic crystals of nonspherical particles," Phys. Rev. B **73**, 035115 (2006).
13. G. Gantzounis, N. Stefanou, and N. Papanikolaou, "Optical properties of periodic structures of metallic nanodisks," Phys. Rev. B **77**, 035101 (2008).
14. C. Tserkezis, N. Papanikolaou, G. Gantzounis, and N. Stefanou, "Understanding artificial optical magnetism of periodic metal-dielectric-metal layered structures," Phys. Rev. B **78**, 165114 (2008).
15. C. Tserkezis, N. Papanikolaou, E. Almpanis, and N. Stefanou, "Tailoring plasmons with metallic nanorod arrays," Phys. Rev. B **80**, 125124 (2009).
16. C. Tserkezis, N. Stefanou, and N. Papanikolaou, "Extraordinary refractive properties of photonic crystals of metallic nanorods," J. Opt. Soc. Am. B **27**, 2620–2627 (2010).
17. A. Christofi, N. Stefanou, G. Gantzounis, and N. Papanikolaou, "Spiral-staircase photonic structures of metallic nanorods," Phys. Rev. B **84**, 125109 (2011).
18. C. Tserkezis and N. Stefanou, "Calculation of waveguide modes in linear chains of metallic nanorods," J. Opt. Soc. Am. B **29**, 827–832 (2012).
19. A. Christofi, N. Stefanou, G. Gantzounis, and N. Papanikolaou, "Giant optical activity of helical architectures of plasmonic nanorods," J. Phys. Chem. C **116**, 16674–16679 (2012).
20. J. D. Jackson, *Classical Electrodynamics*, 3rd ed. (Wiley, 1998).
21. T. J. Garner, A. Lakhtakia, J. K. Breakall, and C. F. Bohren, "Time-domain electromagnetic scattering by a sphere in uniform translational motion," J. Opt. Soc. Am. A **34**, 270–279 (2017).
22. L. Zeng, J. Xu, C. Wang, J. Zhang, Y. Zhao, J. Zeng, and R. Song, "Photonic time crystals," Sci. Rep. **7**, 17165 (2017).
23. T. T. Koutserimpas, A. Alù, and R. Fleury, "Parametric amplification and bidirectional invisibility in PT-symmetric time-Floquet systems," Phys. Rev. A **97**, 013839 (2018).
24. N. Wang, Z.-Q. Zhang, and C. T. Chan, "Photonic Floquet media with a complex time-periodic permittivity," Phys. Rev. B **98**, 085142 (2018).
25. P. A. Pantazopoulos and N. Stefanou, "Layered optomagnonic structures: time Floquet scattering-matrix approach," Phys. Rev. B **99**, 144415 (2019).
26. P. A. Pantazopoulos and N. Stefanou, "Planar optomagnonic cavities driven by surface spin waves," Phys. Rev. B **101**, 134426 (2020).
27. D. L. Sounas and A. Alù, "Non-reciprocal photonics based on time modulation," Nat. Photonics **11**, 774–783 (2017).
28. V. Pacheco-Peña and N. Engheta, "Effective medium concept in temporal metamaterials," Nanophotonics **9**, 379–391 (2020).
29. C. Caloz and Z.-L. Deck-Léger, "Spacetime metamaterials—Part II: theory and applications," IEEE Trans. Antennas Prog. **68**, 1583–1598 (2020).
30. C. Caloz and Z.-L. Deck-Léger, "Spacetime metamaterials—Part I: general concepts," IEEE Trans. Antennas Prog. **68**, 1569–1582 (2020).
31. A. Shaltout, A. Kildishev, and V. Shalaev, "Time-varying metasurfaces and Lorentz non-reciprocity," Opt. Mater. Express **5**, 2459–2467 (2015).
32. N. Chamanara, Y. Vahabzadeh, and C. Caloz, "Simultaneous control of the spatial and temporal spectra of light with space-time varying metasurfaces," IEEE Trans. Antennas Prog. **67**, 2430–2441 (2019).
33. A. M. Shaltout, V. M. Shalaev, and M. L. Brongersma, "Spatiotemporal light control with active metasurfaces," Science **364**, eaat3100 (2019).
34. X. Guo, Y. Ding, Y. Duan, and X. Ni, "Nonreciprocal metasurface with space–time phase modulation," Light Sci. Appl. **8**, 123 (2019).
35. T. T. Koutserimpas and C. Valagiannopoulos, "Multiharmonic resonances of coupled time-modulated resistive metasurfaces," Phys. Rev. Appl. **19**, 064072 (2023).
36. S. Taravati and G. V. Eleftheriades, "Generalized space-time-periodic diffraction gratings: theory and applications," Phys. Rev. Appl. **12**, 024026 (2019).
37. I. Stefanou, P. A. Pantazopoulos, and N. Stefanou, "Light scattering by a spherical particle with a time-periodic refractive index," J. Opt. Soc. Am. B **38**, 407–414 (2021).
38. E. Panagiotidis, E. Almpanis, N. Papanikolaou, and N. Stefanou, "Inelastic light scattering from a dielectric sphere with a time-varying radius," Phys. Rev. A **106**, 013524 (2022).
39. K. Schab, B. Shirley, and K. C. Kerby-Patel, "Scattering properties of spherical time-varying conductive shells," IEEE Trans. Antennas Propag. **70**, 7011–7023 (2022).
40. V. Asadchy, A. Lamprianidis, G. Ptitcyn, M. Albooyeh, Rituraj, T. Karamanos, R. Alaee, S. Tretyakov, C. Rockstuhl, and S. Fan, "Parametric Mie resonances and directional amplification in time-modulated scatterers," Phys. Rev. Appl. **18**, 054065 (2022).
41. G. Ptitcyn, A. Lamprianidis, T. Karamanos, V. Asadchy, R. Alaee, M. Müller, M. Albooyeh, M. S. Mirmoosa, S. Fan, S. Tretyakov, and C. Rockstuhl, "Floquet–Mie theory for time-varying dispersive spheres," Laser Photon. Rev. **17**, 2100683 (2023).
42. M. M. Sadafi, A. F. da Mota, and H. Mosallaei, "Dynamic control of light scattering in a single particle enabled by time modulation," Appl. Phys. Lett. **123**, 101702 (2023).
43. P. Garg, A. G. Lamprianidis, D. Beutel, T. Karamanos, B. Verfürth, and C. Rockstuhl, "Modeling four-dimensional metamaterials: a T-matrix approach to describe time-varying metasurfaces," Opt. Express **30**, 45832–45847 (2022).
44. E. Panagiotidis, E. Almpanis, N. Papanikolaou, and N. Stefanou, "Optical transitions and nonreciprocity in spatio-temporally periodic layers of spherical particles," Adv. Opt. Mater. **11**, 2202812 (2023).
45. T. Inui, Y. Tanabe, and Y. Onodera, *Group Theory and Its Applications in Physics*, Springer Series in Solid-state Sciences (Springer, 1990).
46. G. Gantzounis, "Plasmon modes of axisymmetric metallic nanoparticles: a group theory analysis," J. Phys. Chem. C **113**, 21560–21565 (2009).
47. K. Ohtaka and M. Inoue, "Light scattering from macroscopic spherical bodies. I. Integrated density of states of transverse electromagnetic fields," Phys. Rev. B **25**, 677–688 (1982).
48. G. Sinatkas, T. Christopoulos, O. Tsilipakos, and E. E. Kriezis, "Electro-optic modulation in integrated photonics," J. Appl. Phys. **130**, 010901 (2021).
49. Y. Zhou, M. Z. Alam, M. Karimi, J. Upham, O. Reshef, C. Liu, A. E. Willner, and R. W. Boyd, "Broadband frequency translation through

time refraction in an epsilon-near-zero material," Nat. Commun. **11**, 2180 (2020).
50. E. Lustig, O. Segal, S. Saha, E. Bordo, S. N. Chowdhury, Y. Sharabi, A. Fleischer, A. Boltasseva, O. Cohen, V. M. Shalaev, and M. Segev, "Time-refraction optics with single cycle modulation," Nanophotonics **12**, 2221–2230 (2023).
51. Z. S. Wu and Y. P. Wang, "Electromagnetic scattering for multilayered sphere: recursive algorithms," Radio Sci. **26**, 1393–1401 (1991).
52. I. Gurwich, M. Kleiman, N. Shiloah, and A. Cohen, "Scattering of electromagnetic radiation by multilayered spheroidal particles: recursive procedure," Appl. Opt. **39**, 470–477 (2000).
53. V. G. Farafonov and N. V. Voshchinnikov, "Light scattering by a multilayered spheroidal particle," Appl. Opt. **51**, 1586–1597 (2012).